

developed by Bonaquist et al., (2003). Many researchers have reported that both Witczak and Hirsh models are known to be highly biased at the extreme high and/or low temperatures (Kim et al., 2005, Ceylan et al., 2009a, Ceylan et al., 2009b, Far et al., 2009, Martinez et al., 2009, El-Badawy et al., 2011, Awed et al., 2011, El-Badawy et al., 2012, Khattab et al., 2014, Khattab et al., 2015).

Recently, predictive models using Artificial Neural Networks (ANNs) trained with the same set of parameters used in other popular predictive models, such as Witczak and Hirsh models, are available in literature (Ceylan et al., 2009b). Kim et al., (2011) developed several ANNs models for E^* estimates to be included in the Long Term Pavement Performance (LTPP) Database. These few ANNs studies reported better predictions compared to the regression models.

The main purpose of this research is to compare the prediction accuracy of the modified Witczak, Hirsh, and ANNs models based on laboratory measured E^* data.

NCHRP 1-40D G^* -BASED E^* MODEL (MODIFIED WITCZAK)

This model is a modified version of Bari and Witczak's E^* predictive model originally developed in 2005 (Witczak et al. 2007). It is implemented in MEPDG. The model was based on 7400 E^* measurements from 346 mixtures. It predicts E^* as a function of mix aggregate gradation, mix volumetric properties, frequency of loading and binder complex shear modulus and phase angle. The model form follows a sigmoid function as shown in Equation (1) (Witczak et al. 2007):

$$\log_{10} E^* = 0.02 + 0.758 \left(|G_b^*|^{-0.0009} \right) \times \left(6.8232 - 0.03274\rho_{200} + 0.00431\rho_{200}^2 + 0.0104\rho_4 - 0.00012\rho_4^2 \right) + 0.00678\rho_{38} - 0.00016\rho_{38}^2 - 0.0796V_a - 1.1689 \left(\frac{V_{beff}}{V_a + V_{beff}} \right) + \frac{1.437 + 0.03313V_a + 0.6926 \left(\frac{V_{beff}}{V_a + V_{beff}} \right) + 0.00891\rho_{38} - 0.00007\rho_{38}^2 - 0.0081\rho_{34}}{1 + e^{(-4.5868 - 0.8176 \log |G_b^*| + 3.2738 \log \delta)}} \quad (1)$$

where: E^* =HMA dynamic modulus, in 10^5 psi; $|G_b^*|$ = complex shear modulus of binder, psi; δ = phase angle of the binder, degrees; f = loading frequency, in Hz; V_a = % air voids in the mix, by volume; V_{beff} = % effective binder content, by volume; $\rho_{3/4}$ = % cumulative retained weight on the $3/4$ in. sieve; $\rho_{3/8}$ = % cumulative retained weight on the $3/8$ in. sieve; ρ_4 = % cumulative retained weight on the No.4 sieve; and ρ_{200} = % passing No.200 sieve.

HIRSH MODEL

Christensen et al., (2003) developed an E^* predictive model based upon an existing version of the law of mixtures, called Hirsch model. This model was developed based on 206 E^* measurements from 18 different HMA mixtures containing eight different binders. It is a semi-empirical model that directly relates the dynamic modulus of HMA to the binder shear modulus, voids in mineral aggregate (VMA) and voids filled with asphalt (VFA). The model is given in Equations 2, 3 (Christensen et al., 2003):

$$E^* = Pc \left[4,200,000 \left(1 - \frac{VMA}{100} \right) + 3|G^*| \left(\frac{VFA \times VMA}{10,000} \right) \right] + (1 - Pc) \times \left[\frac{1 - \frac{VMA}{100}}{4,200,000} + \frac{VMA}{3 \times VFA \times |G^*|} \right]^{-1} \quad (2)$$

$$Pc = \frac{\left(20 + \frac{VFA \times 3|G^*|}{VMA} \right)^{0.58}}{650 + \left(\frac{VFA \times 3|G^*|}{VMA} \right)^{0.58}} \quad (3)$$

where: E^* = dynamic modulus of the mixture, in psi; $|G^*| = |G_b^*|$ = shear modulus of the binder, in psi; VMA = % voids in the mineral aggregates; VFA = % voids in mineral aggregates filled with binder; P_c = contact volume computed as given in Equation (3).

INVESTIGATED MIXTURES

A total of 25 Superpave mixes were collected from different ongoing construction projects in the kingdom of Saudi Arabia (KSA). The selected mixes cover the central, northern, southern and, eastern regions of KSA (Khattab et al., 2014, Khattab et al., 2015). Out of the 25 investigated mixes, 14 were mixed in the laboratory (each mix was compacted to achieve 2%, 4%, and 8% air voids), while 11 were plant-produced mixes. These mixes contained 12 mixes with nominal maximum aggregate size (NMAS) of 25 mm and 13 mixes with NMAS of 12.5 mm. The mixes covered fine, medium, and coarse gradations. The investigated mixes contained unmodified and modified binders.

SPECIMEN PREPARATION AND E^* TESTING

Each E^* specimen was compacted using a Controls Gyrotory Compactor (CGC) model ICT 250 to achieve cylinders of 150 mm diameter and 170 mm height. The samples were trimmed from the top and bottom to reach a final height of 150 mm then cored in the middle to produce a final diameter of 100 mm. Three on-specimen vertical LVDT's were used to monitor the axial deformation of each specimen. The E^* tests were conducted according to AASHTO T342-11 at -10, 4.4, 21.1, and 54.4 °C. At each temperature, the tests were conducted at loading frequencies of 25, 10, 5, 1, 0.5, and 0.1 Hz (AASHTO T342, 2011). Hence, 24 dynamic modulus measurements were determined for each sample (4 temperatures and 6 frequencies). Asphalt Mixture Performance Tester (AMPT) was used to run all E^* tests. All tests were conducted at the Ministry of Transport (MOT) Laboratory, General Directorate for Material and Research, Quality Control Department in Riyadh, KSA.

BINDER DYNAMIC SHEAR RHEOMETER TESTING

Dynamic Shear Rheometer (DSR) tests were run on rolling thin film oven (RTFO) aged binders at three test temperatures and 10 rad/sec angular frequency according to AASHTO T315-06 to determine the binder dynamic shear modulus (G_b^*) and phase angle (δ) (AASHTO T315, 2006).

RESULTS AND ANALYSIS

The mixture properties required to run the investigated E^* predictive models are summarized in Table 1. In order to use the two models for E^* prediction at a specific temperature and loading frequency, G_b^* and δ for the binder should be determined at the same temperature and loading frequency of E^* . Since G_b^* and δ for the binder are usually determined in the laboratory over a range of temperatures and only one loading frequency which is 1.59 Hz (10 rad/s) as per the Superpave requirements, the following methodology which is the same used by MEPDG was used to find out the G_b^* and δ at any loading frequency and temperature. First the relationship given by Equation (4) was used to estimate the viscosity at different temperatures as a function of (G_b^*) and (δ) measured by DSR (Witczak et al. 2007).

$$\eta = \left(\frac{G_b^*}{10}\right) \left(\frac{1}{\sin \delta}\right)^{4.8628} \quad (4)$$

where: G_b^* = dynamic shear modulus of binder, psi; η = binder viscosity, in 10^6 poise; and δ = phase angle of the binder, degrees.

Equation (5) was then used to estimate the A and VTS values for each binder.

$$\log \log \eta = A + VTS \log T_R \quad (5)$$

where: η = binder viscosity, in cp; T_R = testing temperature, in Rankine; A = regression intercept; and VTS = regression slope of the viscosity-temperature relationship.

Table 2 lists the A and VTS parameters with the computed coefficient of determination (R^2) values. These values were estimated by fitting the viscosity temperature data for each binder by the linear regression equation given above (Eq. 5) and following the ASTM D2493M-09 method. The R^2 values developed for the A-VTS relationships for all investigated binders ranged from 0.980 to 0.999 indicating excellent linear relationships. Once the A and VTS are determined, Equations (6 to 11) were then used to estimate the binder G_b^* and δ at the temperature and frequency of interest (Witczak et al. 2007):

$$\log \log \eta_{f_s, T} = A' + VTS' \log T_R \quad (6)$$

$$A' = 0.9699 * f_s^{-0.0527} * A \quad (7)$$

$$VTS' = 0.9668 * f_s^{-0.0575} * VTS \quad (8)$$

$$f_s = f_c / 2\pi \quad (9)$$

$$\delta = 90 - 0.1785 * \log(\eta_{f_s, T})^{2.3814} * (f_s)^{(0.3507 + 0.0782VTS')} \quad (10)$$

$$|G_b^*| = 1.469 * 10^{-9} * \log(\eta_{f_s, T})^{12.0056} * f_s^{0.7418} (\sin \delta)^{0.6806} \quad (11)$$

where: f_c = loading frequency in dynamic compression loading as used in the G_b^* testing, in Hz; f_s = loading frequency in dynamic shear loading mode as used in the G_b^* testing, in Hz; A' = adjusted "A" (adjusted for loading frequency); VTS' = adjusted "VTS" (adjusted for loading frequency); $\eta_{f_s, T}$ = binder viscosity as a function of both loading frequency (f_s) and temperature (T_R), in cP; $|G_b^*|$ = complex binder shear modulus, in Pa.

Table 1. Properties of the Investigated Mixtures Required for the E* Models

Mix ID	PG Grade	Mixtures Gradation				V _a %	VMA	VFA	V _{beff}
		$\rho_{3/4''}$	$\rho_{3/8''}$	$\rho_{\#4}$	$\rho_{\#200}$				
T6(F)	64-10	0.0	10.5	38.0	5.6	6.5	14.4	73.8	10.3
T7(F)	76-10	0.0	10.5	38.0	5.6	6.4	14.0	75.0	10.0
T6(M)	64-10	0.0	14.9	43.0	5.2	7.2	14.0	71.1	9.7
T7(M)	76-10	0.0	14.9	43.0	5.2	5.6	14.4	71.0	10.3
T6(C)	64-10	0.0	19.3	50.3	4.6	6.6	14.1	74.3	10.1
T7(C)	76-10	0.0	19.3	50.3	4.6	6.1	14.0	75.0	10.1
H6(C)	64-10	0.0	12.4	37.4	5.2	5.5	15.4	74.3	6.3
H7(C)	76-10	0.0	12.4	37.4	5.2	5.9	15.8	74.3	6.6
H6(M)	64-10	0.0	17.5	45.2	4.8	4.5	15.1	75.9	6.3
H7(M)	76-10	0.0	17.5	45.2	4.8	5.1	15.5	72.6	6.1
H6(F)	64-10	0.0	20.7	51.0	4.4	4.7	15.1	75.1	5.8
H7(F)	76-10	0.0	20.7	51.0	4.4	7.0	15.0	74.9	5.5
FW	70-10	13.4	38.1	48.4	5.7	7.0	12.8	68.3	5.5
HG	70-10	17.0	47.5	62.1	4.2	7.6	12.7	68.2	8.9
NH	76-10	0.0	15.2	37.8	5.0	8.2	15.5	72.3	9.0
SJ	76-10	16.4	47.1	66.4	3.8	8.7	12.9	68.2	11.3
SP	76-10	15.9	35.9	62.0	6.5	7.7	12.9	72.1	7.0
FQ	76-10	23.0	58.2	66.7	3.3	6.3	12.9	68.9	7.4
AJM K	76-10	16.4	50.0	63.5	4.5	6.4	13.9	71.1	7.5
AJMD	76-10	11.3	44.1	62.0	4.3	6.4	13.2	69.9	9.0
AUYN	76-10	12.7	42.0	63.5	5.7	4.8	13.4	68.3	9.6
BIN JAR	70-10	13.0	34.1	59.5	4.3	6.1	13.6	69.0	10.1
HH	70-10	17.8	39.7	56.3	5.3	8.2	13.8	65.5	7.2
A	64-10	17.8	46.9	58.8	4.9	4.4	12.5	65.0	8.6
D	76-10	17.8	46.9	58.8	4.9	4.5	12.4	65.9	8.6

$\rho_{3/4''}$, $\rho_{3/8''}$, $\rho_{\#4}$ = percent retained on sieves 3/4", 3/8", and #4, respectively; $\rho_{\#200}$ = percent passing sieve #200; V_a = percent air voids; (C) = coarse gradation mix; (M) = medium gradation mix; (F) = fine gradation mix; VMA = voids in mineral aggregate; VFA = voids filled with binder; V_{beff} = effective binder content by volume; and PG = binder performance grade.

Table 2. Binder Viscosity-Temperature (A-VTS) Parameters for all RTFO-Aged Binders based on the DSR Results

Mix ID	Binder PG Grade	(DSR@10rad/s)		
		A	VTS	R ²
H,T6 (F&M&C)	64-10	8.815	-2.897	0.995
H,T7 (F&M&C)	76-10	11.680	-3.908	0.998
FW	70-10	8.674	-2.844	0.999
SJ	76-10	8.542	-2.787	0.999
SP	76-10	9.699	-3.200	0.999
HG	70-10	10.200	-3.386	0.999
FQ	76-10	8.542	-2.787	0.999
AJM (K&D)	76-10	9.493	-3.125	0.999
AUYN	76-10	10.060	-3.327	0.999
BIN JAR	70-10	9.590	-3.160	0.999
HH	70-10	9.788	-3.245	0.999
A	64-10	9.501	-3.143	0.997
D	76-10	12.123	-4.065	0.999
NH	76-10	10.916	-3.652	0.980

The established database contains 2592 E^* measurements. This data was used to evaluate the prediction accuracy of modified Witczak and Hirsh models. For the ANNs predictions, the same input variables used in the modified Witczak and then Hirsh E^* predictive models were used with the NeuroSolutions version 5 software for E^* predictions. The 2592 data points were divided randomly into two different subsets: the learning data subset containing 70% of the data points, the testing data subset consisting of 20% of data points and the cross validation data subset containing 10% of data points. Both datasets were normalized within the range of (0.0–1.0) for input and output values to satisfy the sigmoid transfer function range. The trained ANNs were also evaluated using all the 2592 data points to obtain the overall predictive accuracy and compare it with the investigated regression models. After many trials, the best results was found using a four-layered structure composed of one input layer (which contains all the input variables), two hidden layers, and one output layer (predicted E^* values). The feed forward error back propagation ANNs architecture was used in this study. It should be noted that this is the same structure proposed Ceylan et al. (2009b). The (10-30- 30-1) and (9-30- 30-1) architectures were chosen as the best architectures, based on the computed mean square error (MSE), using modified Witczak and Hirsh inputs, respectively.

Figures 1 and 2 depict a comparison between measured and predicted E^* using modified Witczak (FIG. 1a), Hirsh (Fig. 1b), ANNs based on modified Witczak inputs (FIG. 2a), and ANNs based on Hirsh inputs (Fig. 2b), respectively. The figures also show the line of equality along with the unconstrained regression line and goodness of fit statistics. It can be concluded from Figs. 1a and 1b that both modified Witczak and Hirsh models yielded very similar goodness of fit statistics. Moreover, both models yielded relatively biased E^* estimates with Witczak being less biased. The modified Witczak model produced biased E^* estimates at the high and intermediate temperatures whereas Hirsh produced biased E^* estimates at the low and high temperatures. The ANNs model based on the modified Witczak inputs produced

highly accurate results (R^2 of 0.89 and S_e/S_y of 0.34) compared to the modified Witczak (R^2 of 0.82 and S_e/S_y of 0.43) and Hirsh (R^2 of 0.81 and S_e/S_y of 0.43) models. However, as the figures indicate the bias in the predictions was higher especially at the high temperatures. The ANNs predictions based on Hirsh inputs produced very similar goodness of fit statistics to Hirsh with slightly higher bias.

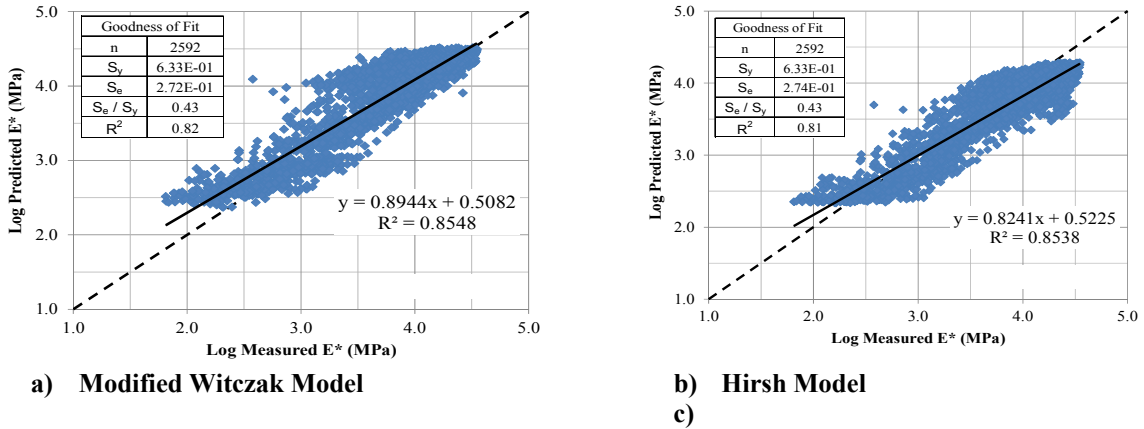


Fig. 1. Comparison of Measured and Predicted E* Values Using Regression.

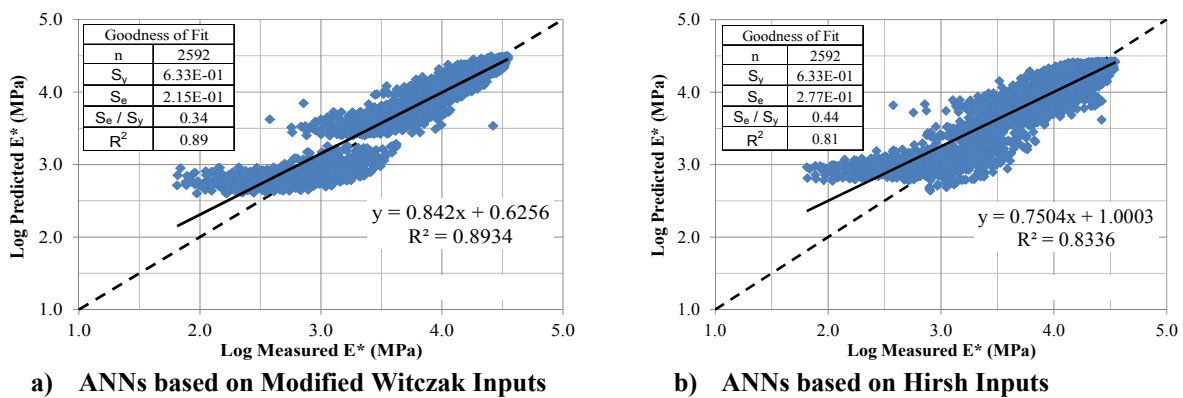


FIG. 2. Comparison of Measured and Predicted E* Values using ANNs.

CONCLUSIONS

A total of 25 Superpave mixes from KSA were tested in the laboratory. The measured E* values of these mixes were compared with the predicted values using modified Witczak, Hirsh and ANNs. This comparison revealed that both the modified Witczak and ANNs model based on modified Witczak inputs yielded the most accurate and least biased E* estimates for the KSA mixes. Hirsh and ANNs based on Hirsh inputs produced accurate but relatively biased predictions at the low and high temperatures. The results of this study suggest that the modified Witczak model and the ANNs based on the modified Witczak models can be used to characterize the KSA mixes. However, caution should be exercised at the low E* values (values at the high temperatures).

ACKNOWLEDGMENTS

Authors acknowledge the technical and financial support provided by Ministry of Transport (MOT) General Directorate for Material and Research, KSA.

REFERENCES

- AASHTO T315-06. (2006). "Standard Method of Test Determining the Rheological Properties of Asphalt Binder Using a Dynamic Shear Rheometer (DSR)." American Association of State Highway and Transportation Officials, Washington, DC.
- AASHTO TP 342-11. (2011). "Standard Method of Test for Determining Dynamic Modulus of Hot Mix Asphalt Concrete Mixtures." American Association of State Highway and Transportation Officials, Washington, DC.
- ASTM D2493M-09. (2009). "Standard Viscosity-Temperature Chart for Asphalts." West Conshohocken, PA.
- Awed, A., El-Badawy, S. and Bayomy F., (2011). "Influence of the MEPDG Binder Characterization Input Level on the Predicted Dynamic Modulus for Idaho Asphalt Concrete Mixtures", Paper No. 11-1268, Presented at the 90th Annual Meeting of the Transportation Research Board and Published in the Annual Meeting DVD, Washington, DC.
- Ceylan, H., Gopalakrishnan, K., and Kim, S., (2009b). "Looking to the Future: The Next Generation Hot Mix Asphalt Dynamic Modulus Prediction Models." *International Journal of Pavement Engineering*, Vol. 10(5): 341-352.
- Ceylan, H., Schwartz, C. W., Kim, S., & Gopalakrishnan, K. (2009a). "Accuracy of Predictive Models for Dynamic Modulus of Hot-Mix Asphalt." *Journal of Materials in Civil Engineering*, 286-293.
- Christensen Jr., D. W., Pellinen, T. K., & Bonaquist, R. F. (2003). "Hirsch Model for Estimating the Modulus of Asphalt Concrete." *Journal of the Association of Asphalt Paving Technologists*. 72:97-121.
- El-Badawy, S., Bayomy, F., and Awed, A., (2011). "Evaluation of the MEPDG Dynamic Modulus Prediction Models for Asphalt Concrete Mixtures", Proceedings of the First Integrated Transportation and Development Institute Congress, Al-Qadi, I., and Murrell, S., Eds., Published by the American Society of Civil Engineers, Chicago, Illinois, USA, 576-585.
- El-Badawy, S., Bayomy, F., and Awed, A., (2012). "Performance of MEPDG Dynamic Modulus Predictive Models for Asphalt Concrete Mixtures — Local Calibration for Idaho." *ASCE's Journal of Materials in Civil Engineering*, 24(11): 1412-1421.
- Far, M., Underwood, B., Ranjithan, S., Kim, R., and Jackson, N. (2009). "Application of Artificial Neural Networks for Estimating Dynamic Modulus of Asphalt Concrete." *Journal of the Transportation Research Board*, No. 2127, Washington, DC, 173-183.
- Garcia, G., and Thompson M. (2007). "HMA Dynamic Modulus Predictive Models-A Review." FHWA-ICT-07-005 Report, Illinois Center for Transportation, University of Illinois, Urbana, IL.

- Khatab, A., El-Badawy, S., Al Hazmi, A., and Elmwafi, M. "Evaluation of Witczak E* Predictive Models for the Implementation of AASHTOWare –Pavement ME Design in the Kingdom of Saudi Arabia", *Construction and Building Materials* V(64) 360-369, Elsevier. doi: 10.1016/j.conbuildmat.2014.04.066.
- Khatab, A., El-Badawy, S., Al Hazmi, A., and Elmwafi, M. (2015). "Comparing Witczak NCHRP 1-40D with Hirsh E* Predictive Models for kingdom of Saudi Arabia Asphalt Mixtures," 3rd Middle East Society of Asphalt Technologists (MEAST): Sustainable Asphalt Pavements in the Middle East, American University of Dubai, United Arab Emirates.
- Kim, Y., R., Underwood, B., Sakhaei Far, M., Jackson, N., and Puccinelli, J., (2007). "LTPP Computed Parameters: Dynamic Modulus," FHWA-HRT-10-035 Final Report, Nichols Consulting Engineers, Chtd.
- Martinez, F. O., and Angelone S. M. (2009). "Evaluation of Different Predictive Dynamic Modulus Models of Asphalt Mixtures used in Argentina." *Bearing Capacity of Roads, Railways, and Airfields*, Tutumluer & Al-Qadi (eds), Taylor & Francis Group, London.
- Witczak, M., El-Basyouny, M., and El-Badawy, S., (2007). "Incorporation of the New (2005) E* Predictive Model in the MEPDG." NCHRP 1-40D Final Report, 2007.

Experimental Study on the Low Temperature Performance of an Epoxy Asphalt Binder and Mixture

Bo Yao¹; Fangchao Li²; and Jianwen Chen³

¹Assistant Professor, Dept. of Civil Engineering, Nanjing Univ. of Science and Technology, 200 Xiaolingwei, Nanjing 210094, P.R. China. E-mail: blade@seu.edu.cn

²Postgraduate, Dept. of Civil Engineering, Nanjing Univ. of Science and Technology, 200 Xiaolingwei, Nanjing 210094, P.R. China. E-mail: lifangchao9999@126.com

³Assistant Professor, Dept. of Civil Engineering, Nanjing Univ. of Science and Technology, 200 Xiaolingwei, Nanjing 210094, P.R. China. E-mail: jianwenchen@njust.edu.cn

Abstract: This paper presents an investigation into the low temperature performance of epoxy asphalt (EA) binder and mixture. The creep characteristics of EA binder at low temperature were determined by the Bending Beam Rheometer test. The Thermal Stress Restrained Specimen Test, bending strength test and bending creep test were utilized to characterize the low temperature performance and cracking resistance of EA mixture. Results showed that the low temperature grade of the EA binder is -16°C according to Superpave performance-graded binder specification. EA mixture exhibits approximately elastic behavior at temperatures below 0°C. The EA mixture shows much higher fracture strength and bending strength along with comparable fracture temperature compared to conventional asphalt mixtures.

INTRODUCTION

In the past years, there has been a growing interest in the application of epoxy asphalt (EA) as a surfacing material on orthotropic steel bridge decks (Cong et al. 2011; Qian et al. 2011). Studies have shown that the EA mixture has high stability and good resistance to permanent deformation (rutting), fatigue cracking and damage from moisture and fuel erosion (Mo et al. 2012; Huang et al. 2003). However, most of the tests were conducted at intermediate or high temperatures, the behaviours of EA binder and mixture at low temperatures are not completely clear yet.

The environment in which an asphalt pavement is placed is one of the most important factors affecting its performance. Thermal or low temperature cracking is a major distress of asphalt pavement in the northern part of China, United States, Canada and other locations that experience severe cold weather. This type of failure can occur as a result of a single severe temperature drop or of multiple cycles of less severe temperature change (thermal fatigue) in combination with embrittlement of the asphalt mixture at low temperatures. It is noted that the use of stiffer asphalt results in material that is fundamentally more “brittle”, leading to more cracking at low temperatures (Zhang et al. 2011). EA is a thermosetting polymer-modified asphalt binder incorporating reactive epoxy resin and curing agent (Cubuk et al. 2009). Researches reveal that at high temperatures the addition of epoxy resin to the asphalt binder significantly reduces its flexibility and produces higher stiffness (Yu et al. 2009). These features can be a negative impact on thermal cracking susceptibility and elevates its risk of thermal cracking when extremely cold weather occurs. Therefore, it is essential to evaluate the low temperature performance of EA before its application in cold climate regions where the prevailing failure mode of asphalt pavement is cracking due to thermally induced stresses.

The primary objective of this research is to evaluate the low temperature performance of EA binder and mixture. To achieve this, both binder and mixture properties were investigated. The Bending Beam Rheometer (BBR) test was conducted on EA binder and the mixture performance tests including the Thermal Stress Restrained Specimen Test (TSRST), bending strength test and bending creep test were utilized to determine the low temperature characteristics of EA mixture.

MATERIALS

The EA is a two-part product blended before use. Part A (used at 14.6% by weight of the binder) consists of an epoxy resin formed from epichlorhydrin and bisphenol-A. Part B (used at 85.4% by weight of the binder) is a mix of asphalt and epoxy cross-linker. Details of the properties of the Part A, Part B and the fully-cured blend are presented in Table 1.

Table 1. Properties of EA

Material	Property	Measured Value	Standard
Part A (Resin)	Viscosity at 23 °C (Pa·s)	14	ASTM D445
	Epoxide Equivalent Weight	185	ASTM D1652
	Flash Point (°C)	221	ASTM D92
Part B (Asphalt and Epoxy Cross-linker)	Viscosity at 100 °C (Pa·s)	0.16	ASTM D2983
	Flash Point (°C)	220	ASTM D92
	Acid Value (mg KOH/g)	52.8	ASTM D664
Fully-cured EA Binder	Tensile Strength at 23 °C (MPa)	2.6	ASTM D412
	Tensile Elongation at 23 °C (%)	285	ASTM D412

The basalt aggregate with a 9.5-mm nominal maximum aggregate size was used for preparing EA mixture specimens. The properties of aggregate are summarized in Table 2. A dense-graded gradation was used and shown in Table 3. The binder content of EA mixture was 6.5% (by weight of the aggregate).

Table 2. Properties of the Basalt Aggregate

Property	Measured Value	Standard
Water Absorption (%)	0.65	ASTM C127
Abrasion Loss (%)	11.5	ASTM C131
Polish Value (%)	0.62	ASTM D3319
Sand Equivalent Value	78	ASTM D2419